Journal of Magnetism and Magnetic Materials 355 (2014) 51–57

Contents lists available at ScienceDirect

Journal of Magnetism and Magnetic Materials

journal homepage: www.elsevier.com/locate/jmmm

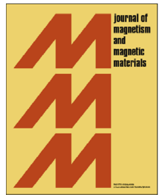

Influences of the type of dopant and substrate on ferromagnetism in ZnO:Mn

Kongping Wu [a,*], Jianhui Jiang [a], Kun Tang [b], Shulin Gu [b,**], Jiandong Ye [b], Shunming Zhu [b], Kailin Lu [a], Mengran Zhou [a], Mingxiang Xu [c], Rong Zhang [b], Youdou Zheng [b]

[a] School of Electrical and Information Engineering, Anhui University of Science and Technology, Huainan, Anhui 232001, People's Republic of China
[b] Nanjing National Laboratory of Microstructures, School of Electronic Science and Engineering, Nanjing University, Nanjing 210093, People's Republic of China
[c] Department of Physics, Southeast University, Nanjing 210096, China

ARTICLE INFO

Article history:
Received 31 July 2013
Received in revised form
20 November 2013
Available online 1 December 2013

Keywords:
Dilute magnetic semiconductor
ZnO template
Magnetization
First principle
ZnO:Mn
Ferromagnetism

ABSTRACT

ZnO:Mn films doped with indium (In) and nitrogen (N) have been grown on sapphire and ZnO template substrates, respectively by the metal-organic chemical vapor deposition method. All these samples show clear hysteresis loops and saturation magnetizations (M_S) at room temperature characterized by a vibrating sample magnetometer in a Quantum Design Physical Property Measurement System. For the - n-type ZnO:(Mn, In) and ZnO:Mn samples, the mechanism of the room-temperature ferromagnetism (RTFM) has been ascribed to the interactions between BMPs, which are formed by the magnetic coupling between Mn ions and the oxygen vacancies (V_O) defects. However, for the p-type ZnO:(Mn, N) samples, a single mechanism is not fully responsible for the measured RTFM. In contrast with the role of V_O in ZnO:(Mn, In) and ZnO:Mn system, the incorporation of V_O in ZnO:(Mn, N) would weaken the FM. For the ZnO:(Mn,N), the observed highest M_S is mainly ascribed to the RKKY interactions from the N 2*p* and Mn 3*d* ferromagnetic exchange coupling. Besides, a density functional theory simulation also indicates that ferromagnetic coupling may be enhanced by V_O in n-type ZnO:(Mn, In) and ZnO:Mn films, while the V_O defects in p-type ZnO:(Mn:N) films act oppositely, that may weaken the ferromagnetic coupling.
© 2013 Elsevier B.V. All rights reserved.

1. Introduction

Diluted magnetic semiconductors (DMSs) have been proposed since two decades ago and have attracted a lot of attention for their potentials in spintronic applications [1], such as logic process, memory storage, communication, and quantum computation [2–4]. After the theoretical prediction of room-temperature (RT) ferromagnetism (FM) in ZnO:Mn by Dietl et al., ZnO doped with magnetic transition metal (TM) ions has been extensively studied. Hundreds of experimental and theoretical papers devoted to the research of FM in ZnO:Mn have been published. However, the origin of the ferromagnetic behavior in ZnO:Mn is still far from being understood. Some research groups [5–7] have claimed that no RTFM exists in ZnO:Mn due to the variations in the crystal structure and oxidation states of the Mn dopants. While some other research groups have reported that the observed FM in ZnO:Mn is intrinsic and induced by the charge carrier's mediated exchange mechanism. For example, RTFM has been reported in ZnO:(Mn, Ga) and ZnO:(Mn, As) samples by Liu and Lim, respectively [8,9].

Furthermore, oxygen vacancy (V_O) defects are broadly recognized as an important reason for interpreting the ferromagnetic behavior of ZnO:Mn. There are experimental evidences [10,11] suggesting that V_O can mediate ferromagnetic coupling. Coey's group reported the role of V_O to obtain FM in ZnO and other oxide systems [12,13]. A few other recent reports also show that the V_O plays a key role in controlling FM in ZnO [14–16].

In the present work, In and N dopants have been introduced into ZnO:Mn by the metal-organic chemical vapor deposition (MOCVD) method. The purpose of the experimental design is to investigate the coupling interaction between charge carriers and Mn local moments. In addition, the role of the V_O defects has been studied based on the analysis of X-ray diffraction (XRD), photoluminescence (PL), and Raman spectra. A theoretical investigation by means of the first principle calculation is finally performed to provide a possible explanation to the role of the V_O.

2. Experiments and numerical simulations

2.1. Preparation of the ZnO:Mn films

Two kinds of substrates were used to grow the ZnO:Mn films. One is the sapphire (0001) substrate, the other is a sapphire

* Corresponding author. Tel./fax: +86 25 83685485.
** Corresponding author.
E-mail addresses: kongpingwu@126.com (K. Wu), slgu@nju.edu.cn (S. Gu).

0304-8853/$ - see front matter © 2013 Elsevier B.V. All rights reserved.
http://dx.doi.org/10.1016/j.jmmm.2013.11.048

substrate with a 3.3-μm-thick ZnO epilayer on it (denoted as ZnO template). The lattice mismatch between sapphire (0001) and ZnO (0001) is around 18.4%, thus the use of the ZnO template as a substrate is to further reduce the mismatch. We hope that the growth of the ZnO:Mn films on the ZnO templates could be a quasi-homoepitaxy that would further improve the quality of the ZnO:Mn films. The ZnO template with a carrier concentration of 0.43×10^{19} cm^{-3} could be referenced in our previous works [17,18].

ZnO:(Mn, In) (sample A), ZnO:Mn (sample B), and ZnO:(Mn, N) (sample C) films were grown at 400 °C in a shower-head MOCVD reactor, which was described in detail elsewhere [19]. One piece of sapphire and one piece of the ZnO template were placed on the substrate holder inside the reactor chamber. The films on the sapphire substrates were denoted as samples A1, B1, and C1, respectively while the ones on the ZnO templates were marked as samples A2, B2, and C2, respectively. During the growth, the diethyl-zinc (DEZn, 99.9998%) and O_2 were employed as Zn metal-organic (MO) precursors and oxidizing source, respectively. The tri-methyl-indium (TMIn, 99.9999%), N_2O and bis (methylcyclopentadienyl) manganese (MCp_2Mn, 99.9998%) were employed to realize In, N, and Mn doping in the ZnO films, respectively. The gas phase concentrations of Mn and In were fixed at 5% and 1%, respectively via tuning the vapor pressure of the MO bubblers and the flow rate of the Ar carrier gas.

2.2. Characterizations

The electrical properties of the ZnO samples were measured by a Hall-effect measurement under van der Pauw's configuration at room temperature. The magnetization vs. magnetic field (*M*–*H*) curves were measured by a vibrating sample magnetometer (VSM) integrated in a physical property measurement system (PPMS-9, Quantum Design) up to 10,000 Oe at room temperature. The nitrogen chemical states were analyzed using an X-ray photoelectron spectroscopy (XPS, Al Kα radiation with the energy of 1486.7 eV, Kratos SAM800). The structural properties were investigated by an XRD ω-2θ scan where a Ni-filtered CuKα ($\lambda = 1.5418 \times 10^{-10}$ m) source was used. The optical properties were characterized by PL with a He–Cd laser as the exciting source with the wavelength of 325 nm and the power of 100 mW. The Raman spectra were recorded using a LabRam micro-Raman spectrometer excited by a 632.8-nm He–Ne laser. All the spectra were taken at room temperature by a grating spectrometer and a photomultiplier detector.

2.3. Super-cell structure and computational details

Our simulations were performed with the Cambridge serial total energy package (CASTEP) code, which is based on the density functional theory using a plane-wave pseudo-potential method [20]. The generalized gradient approximation (GGA) in the scheme of Perdew–Burke–Ernzerhof was used to treat the exchange-correlation function [21]. Besides, the valence-electron configurations for the O, Zn, Mn, N, and In atoms were employed as $2s^2\ 2p^3$, $2s^2\ 2p^4$, $3d^{10}\ 4s^2$, $3d^5\ 4s^2$ and $5s^2\ 5p^1$, respectively. The plane wave functions of valence electrons were expanded by a plane wave basis set. Reciprocal-space integration over the first Brillouin zone was approximated through a careful sampling at a finite number of *k* points using a Monkhorst–Pack mesh [22]. The $2 \times 2 \times 2$ ZnO super cell consisting of 32 atoms was used and the super cell was kept at constant volume. The plane-wave cut-off energy was set to 330 eV and the Hellman–Feynman force components on each ion in the super cell converged at 10^{-3} eV/atom after the convergence test. We then used the Monkhorst–Pack method to establish the super cell (iron impurity model $2 \times 2 \times 2$) and to set *k*-point mesh ($4 \times 4 \times 2$) which guaranteed the convergence of the systematic energy and structure on the quasi-complete plane-wave basis set.

3. Results and discussions

3.1. Characterization results and analysis

Table 1 shows the thickness, resistivity, electron concentration and Hall mobility of the samples grown on sapphire. The ZnO:(Mn, In) shows an n-type conduction with an electron concentration of 1.63×10^{20} cm^{-3}. The high electron concentration is largely due to that the In^{3+} ions substitute for Zn^{2+} sites acting as donors. For the ZnO:Mn film, the electron concentration of 2.03×10^{17} cm^{-3} is mainly due to the deviation from stoichiometry commonly seen in intrinsic ZnO films. For the ZnO:(Mn, N) film, a p-type conduction has been measured with a hole concentration of 4.98×10^{17} cm^{-3}, which indicates that a large number of substituting acceptors (N^{3-} ions substitute for O^{2-} sites) exist in the film. The electrical properties of the films grown on ZnO templates are not shown here because the ZnO template is conductive and thus difficult to extract the real data from the Hall-effect measurement.

The existence of N^{3-} acceptors in the ZnO:(Mn, N) films have been confirmed by XPS. In order to eliminate the surface contamination formed by C and H adsorption, a 20-min Ar^+ ion etching has been done before the XPS spectra were recorded. Chemical bonding states of N in samples C1 and C2 are shown in Fig. 1(a) and (b). A deconvolution of the recorded N 1*s* line has been used for the analysis. It is obvious to see two peaks at 396.5 eV (N1) and 404.5 eV (N2) for both samples. However, another N3 peak at 399.5 eV is essential for a better fitting as shown in Fig. 1(b). The binding energy of peak N1 compares favorably with values found for N^{3-} in metal nitrides, in which the N atom receives substantial charge from the surrounding metal atoms [23]. The peak N2 is typically ascribed to oxygen-rich nitrogen compounds like NO_2^- [23,24]. The additional peak N3 is commonly attributed to amines [25]. The intensity of N1 peak is not attenuated in sample C2 compared to C1, which implies that the form of N^{3-} acceptors also exist in the sample C2. Beside N, other main elements (Zn, O, Mn) also show similar atomic concentrations between samples C1 [O (28.46%), Zn (64.05%), N (1.72%) and Mn (3.37%)] and C2 [O (29.41%), Zn (63.35%), N (1.96%) and Mn (3.43%)], which is determined by the peak intensity integral and normalization. This indicates that the ZnO:(Mn, N) films grown on different substrates should be similar in terms of the chemical composition. The rest percentage comes from carbon and hydrogen impurities unintentionally doped from the MO precursors.

Fig. 2 shows the *M*–*H* curves for all samples, which are obtained by subtracting the contribution from the substrates (shown in the insets of Fig. 2). The shapes of the curves for the substrates indicate that both sapphire substrate and ZnO template have pure diamagnetic behavior, which is consistent with the reports by other research groups [26,27]. After eliminating the effects from the substrates, typical FM hysteresis loops are clearly observed. The saturation magnetization (M_S) values of

Table1
Room-temperature electric properties of samples A1, B1 and C1.

Samples	ZnO:(Mn, In) (A1)	ZnO:Mn (B1)	ZnO:(Mn, N) (C1)
Thickness (μm)	0.45	0.53	0.47
Specific resistance (Ω cm)	0.005	3.987	6.326
Hall mobility (cm^2 V^{-1} s^{-1})	−7.55	−7.69	1.97
Carrier concentration (cm^{-3})	-1.63×10^{20}	-2.03×10^{17}	4.98×10^{17}

Download English Version:

https://daneshyari.com/en/article/1799792

Download Persian Version:

https://daneshyari.com/article/1799792

Daneshyari.com